Effect of a Collector-chimney Junction Model on Solar Chimney Power Plants

Hakim Semai
Centre de Développement des Energies Renouvelables, CDER

Amor Bouhdjar
Centre de Développement des Energies Renouvelables, CDER

Amine Berouaken
Centre de Développement des Energies Renouvelables, CDER

https://doi.org/10.5109/7342474

出版情報：Evergreen. 12 (1), pp.553-563, 2025-03. Interdisciplinary Graduate School of Engineering Sciences, Kyushu University, Japan
バージョン：

Effect of a Collector-chimney Junction Model on Solar Chimney Power Plants

Hakim Semai[1,*], Amor Bouhdjar[1], Amine Berouaken[1,2]

[1]Centre de Développement des Energies Renouvelables, CDER, BP. 62 Route de l'Observatoire, Bouzaréah, Algiers, Algeria

[2]Laboratoire Phénomènes de Transfert, Université des Sciences et de la Technologie Houari Boumediene, USTHB, BP. 32 El-Alia, Bab-Ezzouar, Algiers, Algeria

*Author to whom correspondence should be addressed:
E-mail: hsemai@yahoo.com, h.semai@cder.dz

(Received September 12, 2024; Revised February 18, 2025; Accepted February 26, 2025).

Abstract: A Solar Chimney Power Plant (SCPP) represents an innovative renewable energy technology, though its significant upfront investment cost poses a challenge to widespread adoption.

To address this issue, researchers have explored modifications to the chimney entrance geometry and the implementation of thermal energy storage systems to enhance efficiency and lower costs. This study examined the effects of these modifications on SCPP performance through advanced computational modeling techniques. The study focuses on reducing the tower diameter by 10% and narrowing the flow cross-section at the chimney entrance, along with the implementation of a waterbed for heat storage. The results show that these modifications significantly improve SCPP performance. The reduction in tower diameter and narrowed flow cross-section increase air velocity and power output. Additionally, thermal energy storage enhances energy utilization efficiency, enabling increased power production during nighttime hours and reducing entropy generation. These findings demonstrate the potential of design modifications to enhance SCPP efficiency and cost-effectiveness. By reducing initial investment costs, these improvements can contribute to a wider adoption of SCPPs as a sustainable alternative to conventional fuel systems. This research contributes to global efforts to address energy security and environmental challenges, promoting the shift towards cleaner and more environmentally friendly energy options.

Keywords: heat storage; entropy; natural convection; solar chimney power plant; efficiency

1. Introduction

The growing energy demand and the consequent rise in greenhouse gas emissions, primarily due to fossil fuel consumption, have led to a growing interest in renewable energy sources and their conversion systems. SCPP is one such system that generates green energy using solar power.

The fundamental concept of a SCPP is based on air rising in chimney, caused by the density difference created in solar collector and pressure gradient in the chimney, from the base to the vent. Turbines, positioned inside the chimney inlet (collector-chimney junction), harness the updraft's kinetic energy to generate electricity.

Extensive research has been undertaken on SCPPs, particularly examining how geometric parameters affect system performance[1,2]. The first prototype of a SCPP was experimented by Haaf et al., at Manzanares[3]. In recent years, researchers have increasingly investigated the connection between system efficiency and structural design aspects using both simulation and experimental studies[4]. Nevertheless, there are still numerous areas within this field that lack sufficient research[5,6]. Previous numerical studies have examined how the collector's angle affects chimney efficiency. Substantial alterations in flow parameters, including velocity, pressure, and temperature[7,8] appeared. Moreover, collector power production per unit area increased significantly with inclined collectors and thermal energy storage devices (TES). However, more research is needed to evaluate the collector's inclination angle effect on thermal efficiency, collector performance, and power output[9-12].

Studies have sought to optimize SCPPs based on regional climatic data and structural design aspects[13-15].

The results indicated that larger collector and chimney diameters result in increased air exit velocities, whereas taller collectors negatively affect system performance. Nonetheless, further research is essential to identify the optimal geometric configurations to maximize power output[16].

The chimney's flare angle is another important parameter that influences power output[17]. Computational analyses have revealed that increasing the flare angle reduces the enhancement in power generation. Furthermore, sunlight intensity and chimney radius have a direct impact on power output, with an optimal divergent angle achieving maximum power generation[18].

Comparative research has demonstrated that divergent chimneys surpass cylindrical chimneys in performance, achieving a 54% increase in efficiency[19]. Additionally, chimney divergent angle has been found to affect power output, with a divergence angle of 2 degrees yielding optimal results[20]. Additional research is needed to identify the ideal chimney shape and divergence angle for improved performance.

Impact of TES on SCPP Efficiency, particularly after sunset, requires also further exploration. Research indicates that solar concentrating power plants (SCPPs) equipped with TES outperform those without storage when operating under identical conditions[21].

conducted a study centered on numerical modeling and optimizing the performance of SCPPs by examining different collector ground materials and varying inlet heights[22].

Further research is required to better understand how storage systems affect plant performance and extend operational periods after sunset.

Innovative approaches are being investigated in solar energy, including the development of hybrid systems that utilize solar chimneys to cool photovoltaic (solar) cells[23]. Another approach involves integrating crops within the SCPP, which enhances the system's value and reduces initial costs[24] .

Finally, extensive research on the practical implementation and assessment of medium-scale SCPPs remains limited. While some studies have documented the construction of such plants and their electricity generation processes, further investigation and extensive datasets are necessary to validate the mathematical models put forward by researchers[25].

Given these gaps in research, this study aims to enhance the understanding of SCPPs by conducting computational investigations into different chimney configurations. By addressing the aforementioned research gaps, this study aims to enhance our understanding of SCPPs and their potential as viable sustainable energy solutions.

Regarding the cost of power plants, numerous works have been undertaken to find a balance between the cost and SCPPs performance's. Compared to other clean energy such as wind or solar PVs, the initial construction and maintenance costs of SCPPs can be considerably higher[26]. Pretorius and Kröger[27] conducted a study specifically focused on investigating the optimal configurations of large-scale SCPPs, considering construction costs. Their research identified key dimensions for optimization and resulted in an approximate cost model to determine the ideal plant dimensions for different structure cost. The cost model might estimate the expenses associated with a solar chimney. It is crucial to understand that the purpose of the model was not to provide an exact cost estimation, but rather to offer an initial approximate cost for comparing plant cost with respect to the dimensions. Based on their analysis, the study concluded that large thermos-economically optimal plants were more cost-effective when considering comparable structures cost.

Other studies considered floating chimney or inflatable freestanding flexible solar towers as viable alternatives[28-30]. The great advantage of using a floating chimney is its ability to extend thousands of meters without requiring additional support structures. This flexibility in power plant placement can potentially lower construction costs[31].

PAPAGEORGIOU[26] undertook a comparative study between a concrete tower and a floating chimney. Results revealed that the floating option could be significantly more cost-effective, with a cost that is approximately 5 to 6 times lower than its concrete counterpart is. Furthermore, the required area for the collector came up 4 to 10 times smaller in a floating chimney.

Other authors considered a mountainside supporting the tower chimney[31,32]. Zhou and Yang[31] propose a novel SCPP design featuring a floating chimney structure anchored to a mountainside, aimed at generating electricity in China's desert regions. The design features a large solar collector spread across the desert floor, with a floating chimney attached segmentally to a nearby mountainside. Turbine generators are installed at the chimney's base. Heated air, due to its buoyancy, ascends through the chimney, driving the turbines to generate electricity. The air eventually exits from the top of the chimney. This floating chimney power plant is projected to have a levelized cost of electricity comparable to that of clean coal power plants. Additionally, the novel design can substantially improve SCPP efficiency compared to traditional designs.

The performance of SCPPs is influenced by variations in geometric parameters. For instance, increasing the chimney height leads to increasing the system's power output[33,34]. Similarly, a comparable trend is seen with the collector radius[35]. However, previous studies have indicated that power output remains relatively constant once the collector radius exceeds a certain threshold value[36].

The present work focuses on SCPP's geometric design. Literature on the subject generally considers towers of constant diameter or a conical shape tower[37]. This research examines the tower's narrowing, while in the second scenario, the heat storage system consists of the ground and a water-filled tub placed over it, spanning the entire area beneath the collector. The tub is sealed with a transparent cover to minimize evaporation. Three configurations of the tower are considered with a constant diameter, a constricted flow section at the chimney inlet (at 6m above the ground level), and a constricted flow section at the chimney inlet with a 10% reduction in tower diameter.

2. SCPP Geometry

Figure 1 depicts a 3D scheme of the studied SCPP. It consists of a cylindrical tower that is 200 meters tall with an internal radius of 5 meters (H_{ch} and R_{ch}, respectively). In 4 out of the 6 studied cases, the chimney entrance was modified to have a reduced radius, R_E, of 3 m. The reduced entrance is located 4 m above the canopy which is a flat circular surface with a radius, R_C, of 122 m, and constitutes the collector. The canopy is situated 2 m above the soil level, which allows for a large air circulation flow rate, enhancing the SCPP efficiency, while also providing ample space for agricultural activities in some situation.

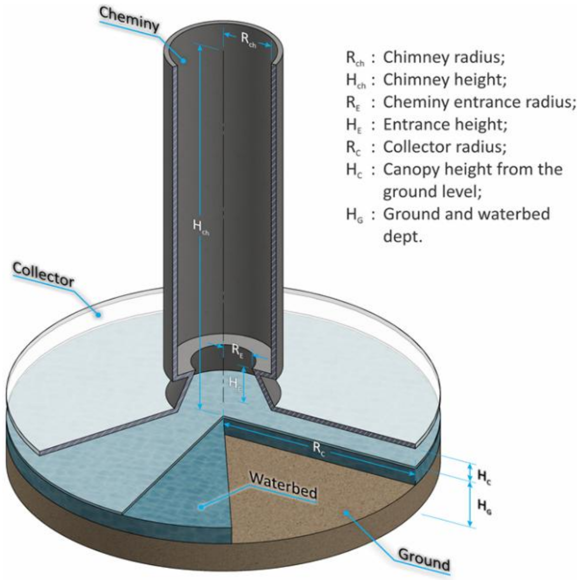

Fig. 1: 3D sectioned view of the modified SCPP.

Six distinct configurations of SCPP are analyzed to evaluate the collective impact of storage media, the reduced entrance, and the tower radius. The configurations can be gathered into two-entrance section. The narrowed section of the entrance tower diameter is evaluated alongside two cases of heat storing systems. In the first scenario, the ground beneath the collector serves as a heat storage medium, leading to reduced entrance SCPPs with varying tower radii. Table 1 gives the geometrical parameters of each configuration.

Table 1. Dimensions of the six configurations of (SCPP).

Configuration	H_{wb} (cm)	R_{ch} (m)	R_{ch}-R_E (m)	H_E (m)
SCPP1	10	5	0	-
SCPP2	10	5	2	4
SCPP3	10	4.5	1.5	4
SCPP4	0	5	0	-
SCPP5	0	5	2	4
SCPP6	0	4.5	1.5	4

Note: H_{wb} stands for waterbed height.

3. Mathematical modeling and boundary conditions

3.1 Governing equations

The Rayleigh number concept is crucial for assessing the buoyancy effects in natural convection within the SCPP. The calculation of the Rayleigh number shows that, within the SCPP system, the air movement is generally turbulent, except at the collector inlet[38]. Equation 1 defines the Rayleigh number as follows:

$$R_a = \frac{g\beta(T_h - T_c){D_h}^3}{\alpha\vartheta} \quad (1)$$

where T_h and T_c represent the highest and lowest temperatures in the system, respectively; D_h is the hydraulic diameter, and α the thermal diffusivity. Boussinesq's approximation is employed to account for changes in air density. Analysis of the flow through the SCPP reveals that, for $Ra>10^{10}$, the airflow becomes turbulent[39]. The fundamental equations of mass, momentum, and energy, along with the k-ε model, are defined by the following equations:

$$\frac{\partial\rho}{\partial t} + \frac{\partial(u_i)}{\partial x_i} = 0 \quad (2)$$

$$\frac{\partial u_i}{\partial t} + u_j\frac{\partial u_i}{\partial x_j} = -\frac{1}{\rho}.\frac{\partial P}{\partial x_i} + \vartheta\left(\frac{\partial^2 u_i}{\partial x_j\,\partial x_j}\right) + \rho f_i \quad (3)$$

$$\frac{\partial}{\partial t}(\rho c_p T) + \frac{\partial}{\partial x_j}(\rho u_j c_p T) = \frac{\partial}{\partial x_j}\left(\lambda\frac{\partial T}{\partial x_j}\right) + T\beta\frac{\partial P}{\partial t} + \emptyset \quad (4)$$

$$\frac{\partial}{\partial t}(\rho k) + \frac{\partial}{\partial x_i}(\rho k u_i) = \frac{\partial}{\partial x_j}\left(\left(\mu + \frac{\mu_t}{\sigma_K}\right)\frac{\partial k}{\partial x_j}\right) + G_K + G_b - \rho\varepsilon + S_K \quad (5)$$

$$\frac{\partial}{\partial t}(\rho\varepsilon) + \frac{\partial}{\partial x_i}(\rho\varepsilon u_i) = \frac{\partial}{\partial x_j}\left(\left(\mu + \frac{\mu_t}{\sigma_\varepsilon}\right)\frac{\partial\varepsilon}{\partial x_j}\right) + C_{1\varepsilon}(G_K + C_{3\varepsilon}G_b) - C_{2\varepsilon}\rho\frac{\varepsilon^2}{K} + S_\varepsilon \quad (6)$$

G_k represents the production of turbulence kinetic energy resulting from the mean velocity gradients, defined by $G_k = -\rho\overline{u_i' u_j'}\frac{\partial u_j}{\partial x_i}$;

G_b denotes the turbulence production caused by buoyancy; $\sigma_k and \sigma_\varepsilon$ are the turbulent Prandtl numbers for $k\ and\ \varepsilon$, respectively; and β the thermal expansion factor; $\beta \approx 1/_T$.

Equations 7 define the electrical power delivered by the system[40)]

$$P_{ele} = \frac{2}{3}\left(\eta\ \eta_{coll}\frac{gH_{tr}}{C_p T_\infty}\right)A_{coll}I_G \quad (7)$$

3.2 Entropy generation

The entropy generation rate is an important factor in determining the system efficiency of the SCPP. It is calculated based on the augmentation in disorder or randomness within the system, caused by process irreversibility. In thermodynamics, entropy production assesses the quantity of energy lost as heat, which cannot be utilized to perform work. The entropy generation rate in the SCPP system is generated by two sources, viscous entropy generation $(\dot{S}_v)$ and thermal entropy generation $(\dot{S}_T)$ [41)]. Understanding the rate of entropy production provides valuable information about system performance and the lost energy as heat.

$$\dot{s}_{gen} = \dot{s}_T + \dot{s}_V = \frac{k}{T^2}\left[\left(\frac{\partial T}{\partial x}\right)^2 + \left(\frac{\partial T}{\partial y}\right)^2 + \left(\frac{\partial T}{\partial z}\right)^2\right] + \frac{\emptyset}{T} \quad (8)$$

$$\emptyset = \mu\left\{\begin{matrix} 2\left[\left(\frac{\partial u}{\partial x}\right)^2 + \left(\frac{\partial v}{\partial y}\right)^2 + \left(\frac{\partial w}{\partial z}\right)^2\right] \\ + \left(\frac{\partial u}{\partial y} + \frac{\partial v}{\partial x}\right)^2 + \left(\frac{\partial u}{\partial z} + \frac{\partial w}{\partial x}\right)^2 + \left(\frac{\partial v}{\partial z} + \frac{\partial w}{\partial y}\right)^2 \end{matrix}\right\} \quad (9)$$

$\emptyset$ is the rate of viscous dissipation per unit of volume.

The total entropy production rate $\dot{S}_{gen}$ is computed as the integral of the local rate across the entire volume V

$$\dot{S}_{gen} = \int_V^1 \dot{s}_{gen} dV \quad (10)$$

3.3 Boundary conditions

Solar chimney system (SCPP) is impacted by various environmental factors, such as solar irradiance and ambient temperature. These factors serve as boundary parameters.

At the collector inlet, the relative static pressure and ambient temperature are taken equal to:

$$p_{r,inlet} = 0,\ T_{inlet} = T_\infty \quad (11)$$

The temperature along the base of the thermal storage layer remains constant, as variations are negligible.

Soil temperatures near the surface fluctuate significantly, while deeper layers (below 0.50 m) exhibit more stable temperatures. Beyond 0.70 m, temperatures remain relatively constant, depending on soil type[42)].

A constant soil temperature of 300K is assumed at 5 meter depth. The heat transfer coefficient for the ground is given by the following relation:

$$U_b = \frac{2b}{\sqrt{\pi t}} \quad (12)$$

in which t represents the time measured starting at midnight.

Equation 13 represents the thermal penetration coefficient

$$b = \sqrt{\lambda \rho C_p} \quad (13)$$

Adiabatic walls and non-slip conditions are applied to the chimney:

$$\begin{bmatrix} \frac{\partial T}{\partial x} \\ u = 0 \\ v = 0 \end{bmatrix} \quad (14)$$

The transparent collector cover, with an average transmissivity coefficient of 0.64, absorbs solar radiation throughout the day.

$$u = 0, v = 0, q = I \quad (15)$$

The shadow of the chimney covers at most during the whole year 2.5% of collector area. This might be considered negligible for the functioning of the power plant.

The thermophysical properties of the air are assumed to be constant at the bulk temperature. Weather data from a typical day at the Adrar site in the southwestern region of Algeria is used for reference, (Fig. 2)[43)].

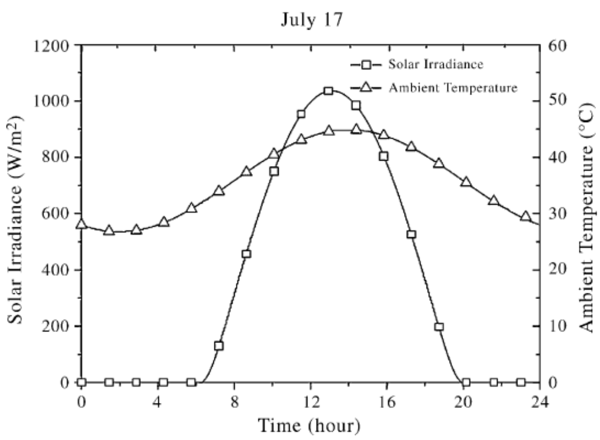

Fig. 2: Solar intensity and ambient temperature on July 17.

4. Numerical method validation

The Manzanares prototype boundary conditions (solar irradiance and ambient temperature on September 2,

1982) and power plant dimensions are used to validate the present code, as used in the validation reference work by Haaf[43]. These findings were then compared with those obtained through numerical calculations. Figure 3 illustrates the air temperature at the wind turbine inlet, showing an average deviation of less than 12% compared to the experimental results of Haaf[44]. Data on air speed at the same location are displayed in Fig. 4. Given the rapid increase and decrease in stack effect caused by external atmospheric factors, values measured before 8:00 AM and after 8:00 PM were discarded. This resulted in an average deviation of no more than 12%. Meanwhile, the deviation obtained for expected power (Fig. 5) was approximately 9%.

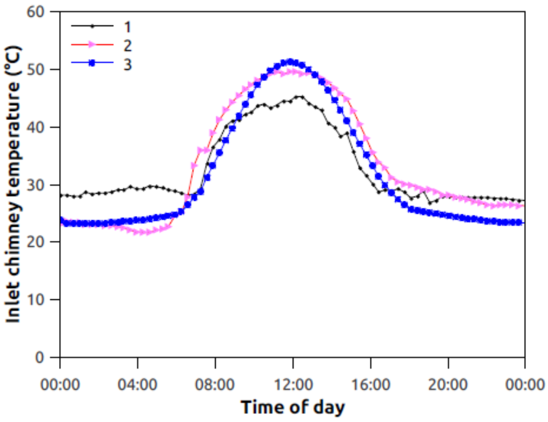

Fig. 3: Inlet chimney temperature, 1- Experimental data[44], 2- Numerical results[45], and 3- Present study results.

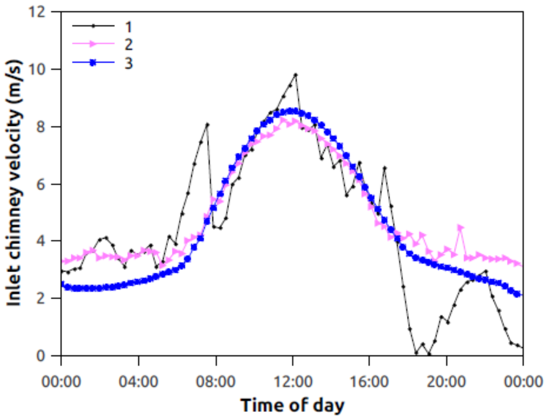

Fig. 4: Inlet chimney velocity over time, 1- Experimental data[44], 2- Numerical results[45], and 3- Present study results.

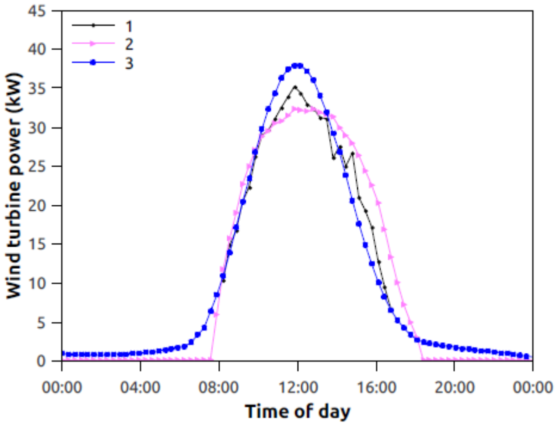

Fig. 5: Power delivered by the wind turbine given by 1- Experimental data[43], 2- Numerical results[44], and 3- Present study results.

A comparison between the results of the current numerical study and those of Hurtado *et al.,*[45] reveals a strong correlation. It is crucial to mention that Hurtado utilized data recorded at the Manzanares prototype[44]. This indicates that the numerical model developed in this research is valid, as it closely matches the experimental data.

5. Simulation results

The SCPP was simulated using the Saturne CFD Code and Syrthes Code. The simulation was designed to represent a typical day in July, with the operational conditions derived from the site's meteorological data. Figure 6 illustrates the velocity profiles for the models that incorporate additional heat storage media. The data show that velocities in all three models (SCPP1, SCPP2, and SCPP3) rise consistently with increasing solar radiation. However, the velocities in the SCPP2 and SCPP3 models are higher during peak solar radiation hours compared to the SCPP1 model. The constricted flow section at the chimney inlet (6 meters above the base) enhances the airflow speed in the SCPP. In particular, the velocity is higher for SCPP3, which features a narrower flow cross-section at the chimney inlet with a 10% reduction in the tower diameter.

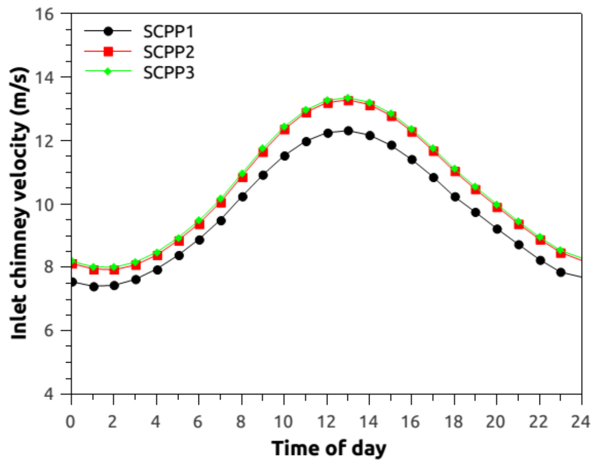

Fig. 6: Mean flow velocity for water storage configuration.

Employing soil as a heat storage medium in the configurations SCPP4, SCPP5, and SCPP6, leads to higher velocities compared to the other models, as seen in Fig. 7. Results are noteworthy for SCPP6. In contrast, using a waterbed as a heat storage medium greatly improves velocity, particularly during times of low solar radiation and after sunset, when compared to systems that rely solely on ground-based heat storage.

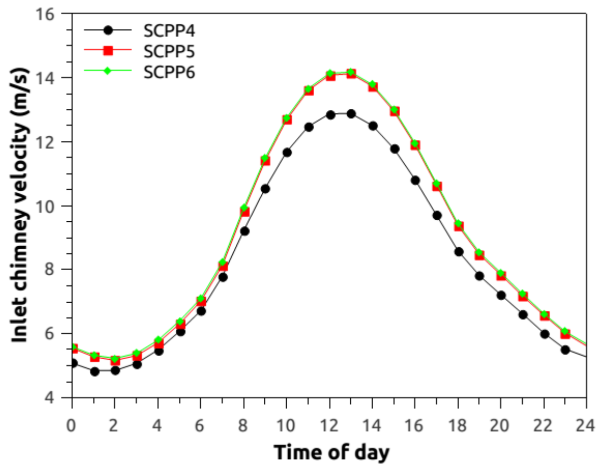

Fig. 7: Mean flow velocity for setups without water heat storage.

As anticipated, the energy production in all configurations increases as solar irradiance rises. However, the maximum generated power is observed in configurations using only the ground as heat storage medium during daytime hours, as illustrated in Fig. 8. Conversely, systems incorporating a waterbed heat storage (SCPP1, SCPP2, and SCPP3) produce a higher amount of power during nighttime hours, as illustrated in Fig. 9.

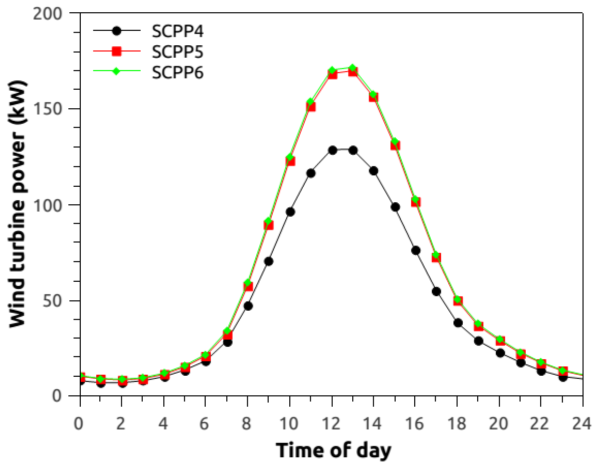

Fig. 8: Power for setups without water heat storage.

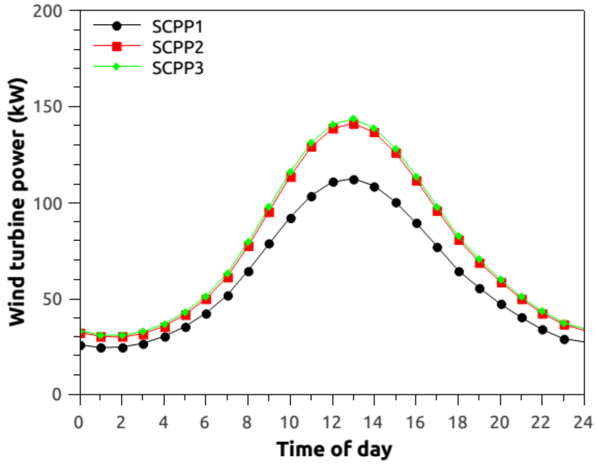

Fig. 9: Power for configurations with water heat storage.

For a similar geometric design, the system that incorporates supplementary heat storage media produces a greater daily yield of electrical energy, as demonstrated in Fig. 10. Among configurations that incorporate waterbed heat storage, the one with a narrowed flow cross-section at the chimney inlet and a 10% reduction in tower diameter (SCPP3) performs optimally for energy production, as illustrated in Fig. 10.

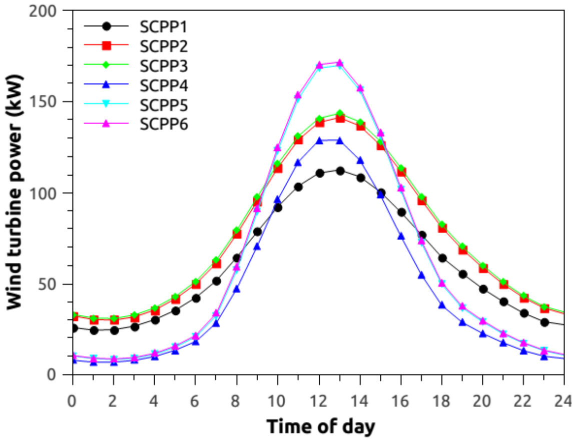

Fig. 10: Power for all configurations during the typical day.

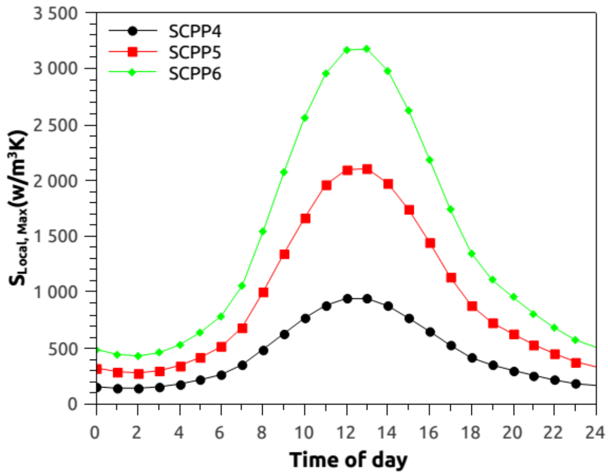

Fig. 12: Local entropy for setups without water heat storage.

Incorporating water-based heat storage into the plant helps minimize fluctuations between peak and low energy production. By absorbing a segment of the incident solar energy and storing it for later use, the waterbed storage increases the overall daily system effectiveness. The system performs efficiently (both day and night), with reduced heat loss attributed to the lower air temperature inside the collector.

Enhancing the SCPP performance is possible through the addition of constriction at the chimney inlet, which increases the electrical power output. This effect is further amplified when combined with heat storage and a reduction of 10% in the tower diameter, as observed for SCPP3.

The thermal gradient between the ground of the collector and the moving air results in a non-equilibrium state within the fluid, causing entropy generation in the system. Achieving an optimal design in thermal systems focuses on reducing this entropy generation.

The findings indicate that, at night, configurations with additional heat storage generate higher levels of local entropy, whereas during the day, configurations without extra heat storage exhibit greater local entropy, with a significant difference (Fig. 11 and 12).

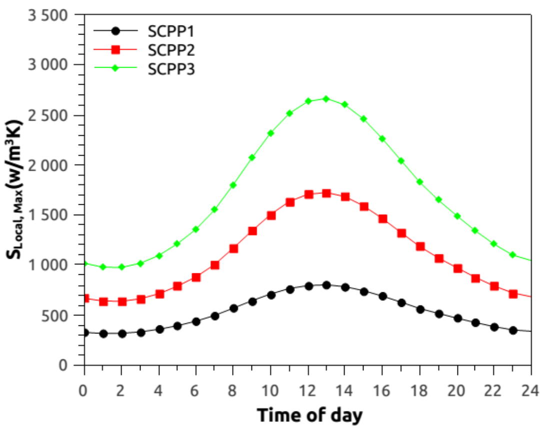

Fig. 11: Local entropy in configurations with water heat storage.

However, total entropy generation remains unchanged for SCPP4 and SCPP5 and is reduced compared to SCPP6 (Fig. 13 and 14). However, configurations incorporating heat storage media show a minimum overall entropy for SCPP1 and SCPP2, while it is slightly higher for SCPP3. Systems with initial tower diameter and those with a restricted flow section at the chimney inlet produce the lowest entropy generation. Conversely, systems with a narrowed flow cross-section at the chimney inlet and a 10% reduction in tower diameter exhibit the highest entropy generation. Configurations with both soil and waterbed storage media generate lower entropy compared to configurations with soil storage only. Thermodynamically, SCPP2 is the optimal configuration for maximizing the fluid's kinetic energy.

However, considering energy production, SCPP3 is the optimal choice, as it generates more electrical energy. Reducing the chimney diameter and, consequently, the turbine blade size can decrease the overall system cost.

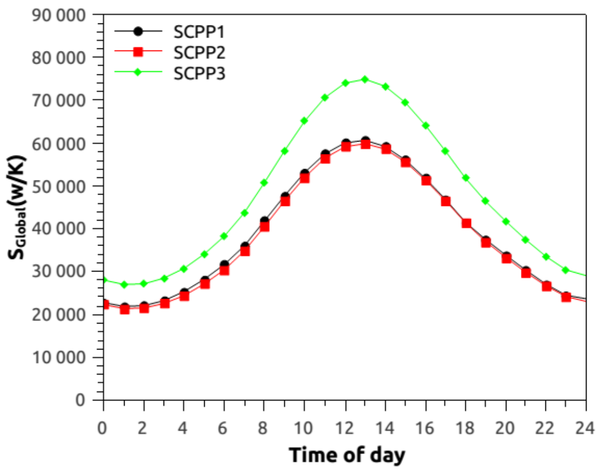

Fig. 13: Global entropy in setups with water storage.

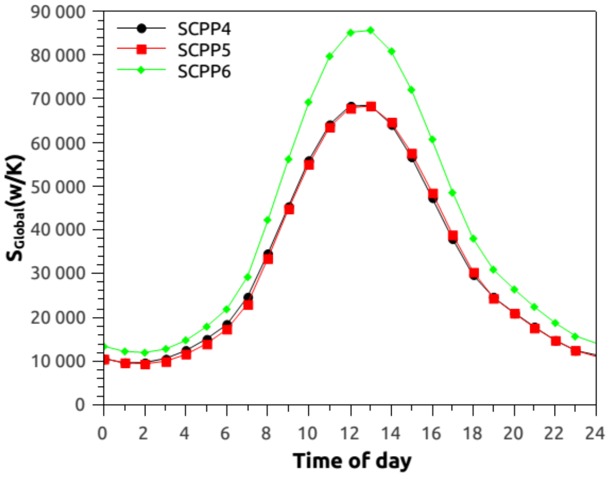

Fig. 14: Global entropy for setups without water heat storage.

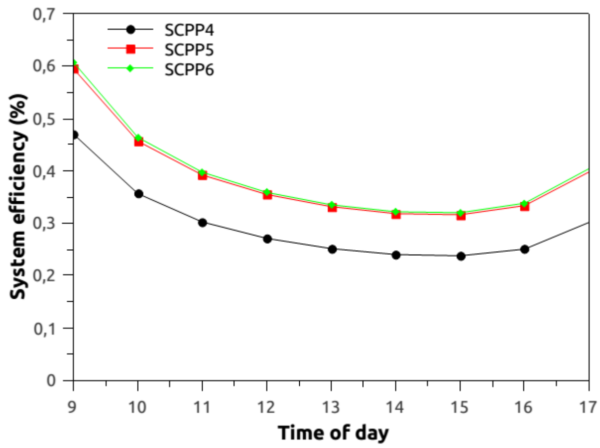

Fig. 16: SCPP's efficiency (without water storage).

Instantaneous plant efficiency (Fig. 15 and 16) is calculated by[45]:

$$\eta_{syst} = \frac{P_{ele}}{I_g A_{coll}} \qquad (16)$$

with IG, the solar irradiance and Acoll, the collector area.

Whether or not additional heat storage media is used, configurations with a narrower flow cross-section at the chimney inlet consistently deliver the best performance. Incorporating additional heat storage significantly improves system efficiency, especially during twilight hours, when the conversion system fully utilizes the stored heat. This results in extended power production even during periods of low sunshine. Overall, systems with additional heat storage demonstrate significantly higher efficiency, with the SCPP3 configuration delivering the best performance, which features a narrowed flow cross-section at the chimney entrance and a 10% reduction in tower diameter.

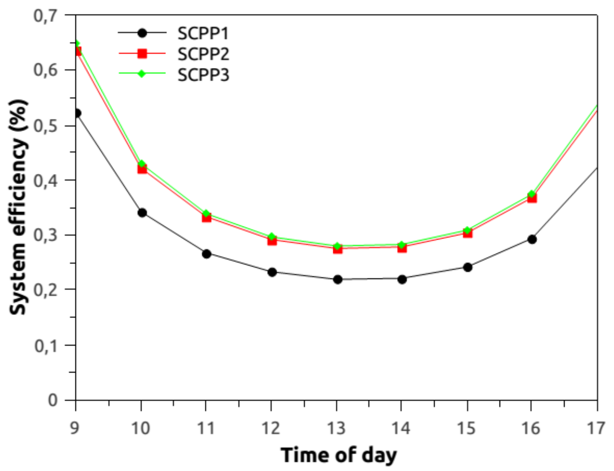

Fig. 15: SCPP's efficiency (with water storage).

6. Conclusion

Numerical simulations were conducted on SCPP using the Saturne and Syrthes codes to analyze how geometrical modifications to the tower affect the plant's performance. Six different configurations were considered, considering a constant tower diameter, a constricted flow section at the chimney inlet, and a narrowed flow cross-section at the chimney inlet with a 10% reduction in tower diameter. Assessment considering factors such as flow speed, generated power, and entropy revealed that the configuration with a narrowed flow cross-section at the chimney entrance provided the best performance, as evidenced by the efficiency results too. To further enhance efficiency and ensure consistent energy production, heat storage media were incorporated into specific configurations. This added heat storage improved the management of collected energy by prolonging its transfer to the moving air, thereby enhancing power output during the night. The results from all six models reveal that:

- The SCPPs can maintain continuous operation throughout the day.
- Solar chimney power plants that rely solely on the ground for thermal storage (SCPP4, SCPP5, and SCPP6) exhibit the highest flow rates. However, after sunset, the highest velocities are achieved in configurations that incorporate additional thermal storage media (SCPP1, SCPP2, and SCPP3).
- The electrical power output during the day is greater in SCPP4, SCPP5 and SCPP6.
- Plants equipped with additional heat storage media (SCPP1, SCPP2, and SCPP3) generate even higher electrical power during the night.
- Models that use only ground as the storage system (SCPP4, SCPP5, and SCPP6) exhibit higher entropy production.
- Four models (SCPP1, SCPP2, SCPP4, and SCPP5) show a reduction in entropy.

Based on these results, the SCPP configuration with a narrowed flow cross-section at the chimney inlet, a 10%

reduction in tower diameter, and extra heat storage media (SCPP3) proved to be the most efficient, providing consistent operation and efficiency throughout the day, while also offering reduced system costs. This configuration ensures uninterrupted operation, which is critical in ensuring a smooth power generation process. Its increased efficiency and electrical power generation, along with the extra heat storage media, make it cost-effective and an attractive option for stakeholders seeking efficient energy production solutions.

Nomenclature

A	area (m^2)
C	sensible heat flux density $(w.m^{-2})$
c_p	heat capacity per unit mass $(\mathrm{j.kg^{-1}k^{-1}})$
D_h	hydraulic diameter (m)
f	body forces$(\mathrm{kg.m^{-2}.s^{-2}})$
g	gravitational acceleration $(\mathrm{m.s^{-2}})$
H_{ch}	height of chimney (m)
h	heat transfer factor $(w.m^{-2}.K^{-1})$
K	turbulent kinetic energy $(\mathrm{j.kg^{-1}}.m.s^{-2})$
L	length scale(m)
P	pressure (pa)
R	Solaire irradiance $(w.m^{-2})$
Ra	Rayleigh number
$S_{w,p}$	source term (W)
T	temperature (k)
u, v and w	components of velocity $(\mathrm{m.s^{-1}})$

Greek symbols

λ	thermal conductivity $(\mathrm{W.M^{-1}.K^{-1}})$
ΔT	temperature difference (K)
Δp	chimney pressure variation (Pa)
ρ	volumetric density $(kg.m^{-3})$
α	thermal diffusivity $(\mathrm{M^2.S^{-1}})$
v	kinematic viscosity $(\mathrm{M^{-2}.S^{-1}})$
ε	turbulent dissipation rate $(\mathrm{M^2.S^{-3}})$
μ	dynamic viscosity $(\mathrm{Kg.M^{-1}.S^{-1}})$
β	thermal expansion rate $(\mathrm{K^{-1}})$
∅	energy dissipation (W)
η	efficiency

Subscripts

a	air
b	ground
c	cold
ch	chimney
$coll$	collector
$elec$	electric
max	maximum
min	minimum
t	total
∞	environment

References

1) Jawad, A., et al., "Experimental Investigation on The Effect of Divergent Tower Solar Chimney on The Theoretical Power Potential. *Journal of Advanced Research in Fluid Mechanics and Thermal Sciences*", 81(1) 140-149 (2021). doi: 10.37934/arfmts.81.1.140149
2) Azwadi, J.H.Y.T.a.C.S.N., "Numerical Analysis for Optimizing Solar Updraft Tower Design Using Computational Fluid Dynamics (CFD). *Journal of Advanced Research in Fluid Mechanics and Thermal Sciences* ", 22(1) 8-36 (2016).
3) Haaf, W., et al., "Solar Chimneys Part I: Principle and Construction of the Pilot Plant in Manzanares. *International Journal of Solar Energy*", 2(1) 3-20 (2007). doi: 10.1080/01425918308909911
4) Husam Abdulrasool Hasan, K.S., Kayser Aziz Ameen, "Design and Optimizing of Geometric for Solar Updraft Tower using Computational Fluid Dynamics (CFD). *Journal of Advanced Research in Fluid Mechanics and Thermal Sciences*", 51(1) 71-79 (2018).
5) Mehranfar, S., et al., "Comparative assessment of innovative methods to improve solar chimney power plant efficiency. *Sustainable Energy Technologies and Assessments*", 49 101807 (2022). doi: 10.1016/j.seta.2021.101807
6) Khadersab Adamsab, E.V., Abdulhamid Hamdan Al-Hinai, "An Experimental Investigation of a Small-scale Solar Updraft Tower in the Sultanate of Oman. *Journal of Advanced Research in Fluid Mechanics and Thermal Sciences*", 93(1) 212-221 (2022). doi:10.37934/arfmts.93.1.212221
7) Das, P. and V.P. Chandramohan, "Estimation of flow parameters and power potential of solar vortex engine (SVE) by varying its geometrical configurations: A numerical study. *Energy Conversion and Management*", 223 113272 (2020). doi: 10.1016/j.enconman.2020.113272
8) Semai, H., A. Bouhdjar, and S. Larbi, "Canopy slope effect on the performance of the solar chimney power plant. *International Journal of Green Energy*", 14(3) 229-238 (2016). doi: 10.1080/15435075.2016.1253580
9) Ayadi, A., et al., "Effect of the number of turbine blades on the air flow within a solar chimney power plant. *Proceedings of the Institution of Mechanical Engineers, Part A: Journal of Power and Energy*", 232(4) 425-436 (2017). doi: 10.1177/0957650917733128
10) Keshari, S.R., C. V.P, and P. Das, "A 3D numerical

study to evaluate optimum collector inclination angle of Manzanares solar updraft tower power plant. *Solar Energy*", 226 455-467 (2021). doi: 10.1016/j.solener.2021.08.062

11) Das, P. and V.P. Chandramohan, "3D numerical study on estimating flow and performance parameters of solar updraft tower (SUT) plant: Impact of divergent angle of chimney, ambient temperature, solar flux and turbine efficiency. *Journal of Cleaner Production*", 256 120353 (2020). doi: 10.1016/j.jclepro.2020.120353
12) Safer Nabil, B., "The Effect of The Inclusion of The Secondary Roof Under the Main Roof on Performance of Chimney Solar Power Plants. *Journal of Advanced Research in Fluid Mechanics and Thermal Sciences*", 98 (1) 157-170 (2022). doi: 10.37934/arfmts.98.1.157170
13) S. Larbi, A.B., and T. Chergui, "Performance analysis of a solar chimney power plant in the southwestern region of Algeria. *Renewable and Sustainable Energy Reviews*", 14 (1) 470-477 (2010). doi: 10.1016/j.rser.2009.07.031
14) Badis Bakri, H.B., Haythem Nasraoui, Zied Driss, "Experimental Study of Solar Chimney Power Plant. *Journal of Advanced Research in Fluid Mechanics and Thermal Sciences*", 101(1) 207-214 (2023). doi:10.37934/arfmts.101.1.207214
15) Eugene, V., A. Khadersab, and A.-H. Abdulhamid Hamdan, "Performance Analysis of a Commercial Scale Solar Chimney Power Plant in Oman. *Journal of Advanced Research in Fluid Mechanics and Thermal Sciences*", 96 (1) 1-10 (2022). doi: 10.37934/arfmts.96.1.110
16) Hooi, L.B. and S.K. Thangavelu, "A parametric simulation of solar chimney power plant. *IOP Conference Series: Materials Science and Engineering*", 297 012057 (2018). doi: 10.1088/1757-899x/297/1/012057
17) Semai, H. and A. Bouhdjar, "Impact of the chimney geometry on the power output of solar chimney power plant. *Thermophysics and Aeromechanics*", 28 (2) 291-303 (2021). doi: 10.1134/s0869864321020128
18) Ridwan, A., H. Hafizh, and M.R. Fauzi, "Design and experimental test for solar chimney power plant: case study in Riau Province, Indonesia. *IOP Conference Series: Materials Science and Engineering*", 403 012092 (2018). doi: 10.1088/1757-899x/403/1/012092
19) Ganguli, A., S. Deshpande, and A. Pandit, "CFD Simulations for Performance Enhancement of a Solar Chimney Power Plant (SCPP) and Techno-Economic Feasibility for a 5 MW SCPP in an Indian Context. *Energies*", 14 (11) 3342 (2021). doi: 10.3390/en14113342
20) Natarajan, R., V. Jayaraman, and R. Sathyamurthy, "Comparative studies on performance of solar towers with variable scale ratios. *Environ Sci Pollut Res Int*", 29 (30) 45601-45611.(2022). doi: 10.1007/s11356-022-19079-0
21) Sundararaj, M., et al., "Parametric optimization of novel solar chimney power plant using response surface methodology. *Results in Engineering*", 16 100633 (2022). doi: 10.1016/j.rineng.2022.100633
22) Abdulhamid Hamdan Al-Hinai, K.A., Eugene Vega, "Numerical Investigation of Solar Updraft Tower for Different Collector Inlet Heights and Absorber Materials. *CFD Letters*", 14 (6) 72-78 (2022). doi: 10.37934/cfdl.14.6.7278
23) Hussein A. Jaffar, A.A.I., Ahlam Luaibi Shuraiji, "Review of Hybrid Photovoltaic- Air Updraft Solar Application: Present and Proposed state Models. *EVERGREEN*, 9 (4) 1181-1202 (2022). doi:10.5109/6625729
24) Bouhdjar, H.S.a.A., "Incorporating Vegetation in Solar Chimney Power Plant: A Northern Algerian Site Study. *EVERGREEN*, 11 (2) 846-861 (2024). doi:10.5109/7183365
25) Balijepalli, R., et al., "Numerical analysis on flow and performance characteristics of a small-scale solar updraft tower (SUT) with horizontal absorber plate and collector glass. *Journal of Thermal Analysis and Calorimetry*", 141 (6) 2463-2474 (2020). doi: 10.1007/s10973-020-10057-7
26) PAPAGEORGIOU, C.D., "Floating Solar Chimney versus Concrete Solar Chimney Power Plants (2007). doi: 10.1109/ICCEP.2007.384299
27) Pretorius, J.P. and D.G. Kröger, "Thermoeconomic Optimization of a Solar Chimney Power Plant. *Journal of Solar Energy Engineering*", 130 (2) (2008). doi: 10.1115/1.2840571
28) Zhou, X., et al., "Economic analysis of power generation from floating solar chimney power plant. *Renewable and Sustainable Energy Reviews*", 13 (4) 736-749 (2009). doi: 10.1016/j.rser.2008.02.011
29) Md. Abdul Aziz Bhuiyan, M.H.B., Md. Ashiqur Rahman, Md Atreher Abir, Nagib Mehfuz, Sayedus Salehin, *Economic Assessment of Concrete and Floating Based Solar Chimney Power Plants in Bangladesh*, in *2020 IEEE Region 10 Symposium (TENSYMP)*(2020): Dhaka, Bangladesh.
30) Maghrebi, M.J. and R. Masoudi Nejad, "Performance evaluation of floating solar chimney power plant in Iran: estimation of technology progression and cost investigation. *IET Renewable Power Generation*", 11 (13) 1659-1666 (2017). doi: 10.1049/iet-rpg.2016.0963
31) Zhou, X. and J. Yang, "A Novel Solar Thermal Power Plant with Floating Chimney Stiffened onto a Mountainside and Potential of the Power Generation in China's Deserts. *Heat Transfer Engineering*", 30 (5) 400-407 (2009). doi: 10.1080/01457630802414813
32) Serag-Eldin, M.A., "Analysis of a new solar chimney plant design for mountainous regions. 1 437-446 (2006). doi: 10.2495/ht060421

33) Li, J., H. Guo, and S. Huang, "Power generation quality analysis and geometric optimization for solar chimney power plants. *Solar Energy*", 139 228-237 (2016). doi: 10.1016/j.solener.2016.09.033
34) Ngala GM, O.M., Muhammad AB, Shuwa M, "Evaluation of solar chimney power plant in semi-arid region of Nigeria. *Arid Zone J Eng Technol Environ*", 11 1-12 (2015).
35) Tingzhen, M., L. Wei, and X. Guoliang, "Analytical and numerical investigation of the solar chimney power plant systems. *International Journal of Energy Research*", 30 (11) 861-873 (2006). doi: 10.1002/er.1191
36) Li, J.-y., P.-h. Guo, and Y. Wang, "Effects of collector radius and chimney height on power output of a solar chimney power plant with turbines. *Renewable Energy*", 47 21-28 (2012). doi: 10.1016/j.renene.2012.03.018
37) Hu, S., et al., "Effect of guide wall on the potential of a solar chimney power plant. *Renewable Energy*", 96 209-219 (2016). doi: 10.1016/j.renene.2016.04.040
38) Padhi, B.N., M. Pandey, and I. Mishra, "Relation of change in geometrical parameters in the thermal performance of solar chimney. *Journal of Mechanical Science and Technology*", 35(10) 4737-4746 (2021). doi: 10.1007/s12206-021-0939-8
39) Ming, T., et al., "Numerical analysis of flow and heat transfer characteristics in solar chimney power plants with energy storage layer. *Energy Conversion and Management*", 49(10) 2872-2879 (2008). doi: 10.1016/j.enconman.2008.03.004
40) Koonsrisuk, A., "Mathematical modeling of sloped solar chimney power plants. *Energy*", 47(1) 582-589 (2012). doi: 10.1016/j.energy.2012.09.039
41) Ming, T., et al., "Numerical analysis on the influence of ambient crosswind on the performance of solar updraft power plant system. *Renewable and Sustainable Energy Reviews*", 16 (8) 5567-5583 (2012). doi: 10.1016/j.rser.2012.04.055
42) Bezari, S., et al., "Investigation and Analysis of Soil Temperature under Solar Greenhouse Conditions in a Semi-Arid Region. *International Journal of Design & Nature and Ecodynamics*", 17 (3) 325-332 (2022). doi: 10.18280/ijdne.170301
43) Michel, C., *Atlas solaire de l'Algérie Tome 2 : Aspect énergétique*. Vol. 2. 1985. 399.
44) Haaf, W., "Solar Chimneys Part II_ Preliminary Test Results from the Manzanares Pilot Plant. *International Journal of Solar Energy*", 2 (2) 141-161 (2007). doi: 10.1080/01425918408909921
45) Hurtado, F.J., A.S. Kaiser, and B. Zamora, "Evaluation of the influence of soil thermal inertia on the performance of a solar chimney power plant. *Energy*", 47 (1) 213-224 (2012). doi: 10.1016/j.energy.2012.09.040